Grid-Connected Wind Photovoltaic Hybrid Power Systems with GRNN and RBFNSM

Moholkar shreya[1], Ghutke Pratik [2], Wakte Ganesh[3]

[1] Electrical Engineering, Student, TGPCET Nagpur, India. moholkarshreya@gmail.com,
[2] Electrical Engineering, Assistant Professor TGPCET Nagpur, India. pcghutke2214@gmail.com
[3] Electrical Engineering, Assistant Professor TGPCET Nagpur India. ganeswakte1989@gmail.com

ABSTRACT

This work proposes a grid-connected wind-photovoltaic (PV) hybrid power system, as well as the system's steady-state model analysis and control method. PV power, wind power, and an intelligent power controller make up the system. The General Regression Neural Network (GRNN) algorithm was used to examine the performance of a PV generation system with non-linear characteristics. The turbine speed is calculated using a high-performance on-line training radial basis function network-sliding mode (RBFNSM) method to capture maximum power from the wind. The intelligent controller consists of an RBFNSM and a GRNN for maximum power point tracking (MPPT) control to achieve a fast and stable response for power control. The wind turbine pitch angle is regulated by RBFNSM, and the PV system is controlled by GRNN, with the output signal controlling the boost converters to achieve the MPPT. The simulation results show that using MPPT, the suggested hybrid generation system may achieve high efficiency.

Keywords: Maximum power point tracking (MPPT), Photovoltaic (PV), Wind turbine, Hybrid power system, Radial basis function network system model (RBFNSM), General Regression Neural Network (GRNN).

INTRODUCTION

With rising energy consumption and concerns about environmental degradation around the world, renewable energy solutions are becoming increasingly popular. The characteristics of wind energy and photovoltaic energy are complimentary. Combining wind and photovoltaic energy in one system (hybrid system) improves the system's reliability and minimizes the need for storage batteries [1]. The system's main benefit is that it meets the basic power needs of non-electrified rural places where grid power has yet to arrive. The energy generated by the wind and solar panels is stored in a battery bank and can be used anytime it is needed. A hybrid renewable energy system combines two or more energy generation technologies, most commonly solar and wind. The fundamental benefit of a solar/wind hybrid system is that it improves the system's reliability by combining solar and wind power generation. Additionally, because there is less reliance on one form of power generation, the amount of battery storage can be reduced slightly. When the sun isn't shining, there's usually a lot of wind. When the sun's resources are at their peak (summer, eventually), wind speeds are generally low. The wind, on the other hand, is generally stronger during seasons (primarily the winter) when there are fewer sun resources. There are various and opposing patterns in terms of wind and solar resources even on the same day, in many places throughout the world, or at different times of the year.

And because of these various patterns, hybrid systems may be the greatest solution for electricity generation. Large wind and solar PV systems are proportionally cheaper than smaller systems; hence a hybrid wind–solar electric system requires a higher initial investment than single larger systems.

PV power is typically generated using a series of PV panels and a power converter. Adjusting the converter allows you to track the maximum power point of your PV panels. Throughout the years, various MPPT techniques for PV power generation have been presented.

The perturbation and observation method (P&O) [2], power matching, incremental conductance, hill- climbing search, power differential feedback control, curve fitting, dc-link capacitor droop control, intelligent control, and several more special control methods are among these methods.

Because of its simplicity and system independence, the P&O method is used by the majority of studies. Novel methods, such as the optimum gradient method, fuzzy logic control (FLC), and neural networks, are being developed with improved accuracy but a more complex procedure (NN). These techniques may also be expensive, difficult to deploy, and insufficiently stable. The General Regression Neural Network (GRNN) has been used in a variety of systems control and identification applications. Compared to rival algorithms, this algorithm has a lot of advantages. GRNN is a one- pass learning technique with a highly parallel structure that is nonparametric. It makes no assumptions about the underlying distribution's shape.

Other known algorithms are more complicated than GRNN. The suggested approach has the advantage of being very simple to implement, as it does not involve any trial-and-error or prior knowledge of the parameters. Tip speed ratio (TSR) control, power signal feedback (PSF) control, and hill-climb searching (HCS) control are three types of maximum wind power extraction methods that have been studied previously. TSR control adjusts the rotor speed of wind turbines in order to maintain a high TSR. PSF control necessitates knowledge of the wind turbine's maximum power curve, which it tracks using its control mechanisms.

The TSR direction control method [3] is limited among previously developed wind turbine MPPT strategies due to the difficulty in measuring wind speed

and turbine speed. The Radial Basis Function Network (RBFN) has the ability to approximate any complicated nonlinearity infinitely, in addition to parallel computing, learning, and fault tolerance. Sliding mode variable structure control is a nonlinear control strategy with strong robustness against parameter changes, load disturbances, and system uncertainty, as well as the advantages of rapidity and ease of implementation.

The combination of a neural network and sliding mode variable control not only has high robustness, allowing it to withstand system perturbation and external interference, but it also eliminates buffeting. A RBFNSM-based TSR MPPT strategy for wind turbine generators is proposed in this paper. Some research has been done on hybrid systems. A wind turbine system model was developed and compared to a real system in [4, which looked at the dynamic performance of a stand-alone wind– solar system with battery storage. The steady-state performance of a grid-connected wind and PV system with battery storage was analysed in order to propose methodologies for optimal design or unit sizing of stand-alone or grid-connected hybrid systems [5–7].

There are two branches to wind-PV hybrid power generation: wind power generation and PV power generation. Because wind and PV power can partially compensate for each other during the day and night, the development of wind-PV hybrid power generation is appealing. The interface between the hybrid generation system and the power grid must be specially designed for the grid- connected system, which requires expensive hardware and complex control. The hybrid generation system can be easily set up in remote and isolated areas where a connection to the utility network is either impossible or prohibitively expensive for the stand-alone off-grid system.

1. SYSTEM COMPONENT CHARACTERISTIC

Figure 1 depicts the system component characteristics of the proposed wind and PV hybrid system. MATLAB/Simulink was used to create dynamic models of the main components, which included the wind energy conversion system (WECS), PV generation systems, load, and grid.
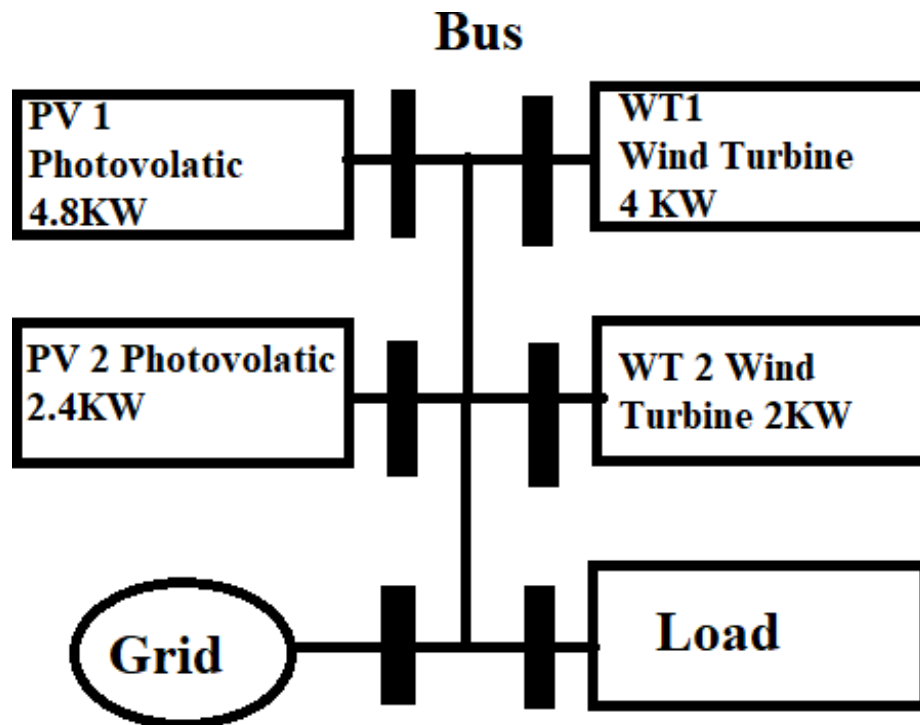

Figure 1 shows a hybrid micro-grid power system that has been proposed.

1.1 Wind turbine

It is necessary to install power electronic devices between the wind turbine generator (WTG) and the grid where the frequency is constant in order to capture the maximum amount of wind energy. The wind is the input to a wind turbine, and the mechanical power that turns the generator rotor is the output [8]. The output mechanical power available from a wind turbine for a variable speed wind turbine could be expressed as

$$P_m = \frac{1}{2}\rho A C_p(\lambda, \beta) V_{\omega}^3$$

The air density and the area swept by blades, respectively, are q and A. Vx is the wind speed in metres per second (m/s), and Cp is the power coefficient, which is defined as a nonlinear function of the tip speed ratio (TSR) k.

$$\lambda = \frac{\omega_r r}{V_\omega}$$

where r is wind turbine blade radius, and xr is the turbine speed. Cp is a function of k and the blade pitch angle b. In this paper, a variable-speed pitch-regulated wind turbine is considered, with the pitch angle controller playing a key role. The groups of Cp k curves of the wind turbine used in this study at various pitch angles are shown in Fig. 2 [9]. Cp can be changed by adjusting the pitch angle, as shown in the diagram (b). In other words, pitch angle control can control the wind turbine's output power. PV cell conventional model (2.2) The circuit equivalent of a PV cell is shown in Figure 3. The PV cell's equivalent equation is as follows [6]:

$$V_{PV} = \frac{nKT}{q} \ln \left(\frac{I_{ph}}{I_{pv}} + 1 \right)$$

$$I_{PV} = I_{ph} - I_{PVO} \left[\exp \left(\frac{q(V_{PV} + I_{pv}R_s)}{nKT} \right) - 1 \right] - \frac{V_{PV} + R_s I_{PV}}{R_{sh}}$$

Series and shunt resistances (X) are represented by Rs and Rsh, respectively. Iph is the PV Cell's photocurrent (A), n is the p–n junction's ideality factor, IPVO is the reverse saturation current (A), K is the Boltzmann constant (1.38 10 23 J/K), q is the electronic charge (1.602 10 19 C), and T is the cell's temperature (K).
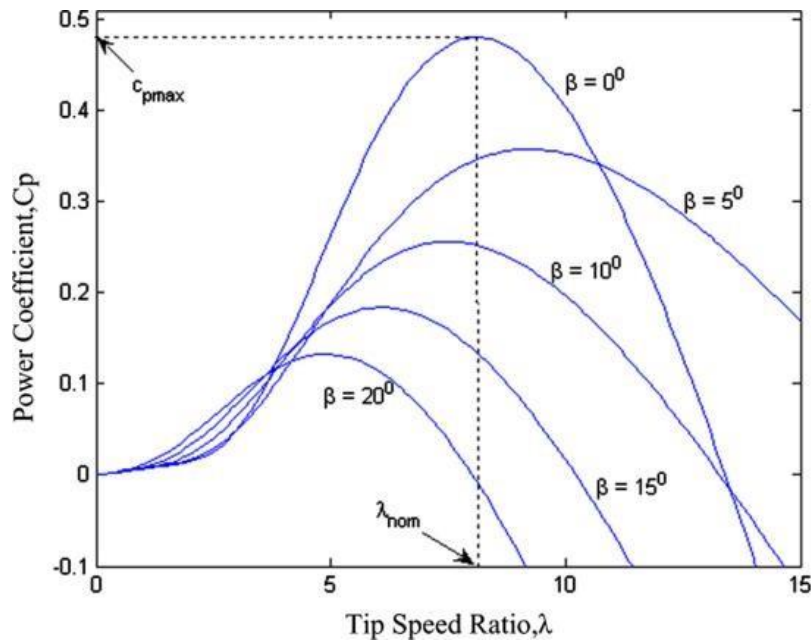

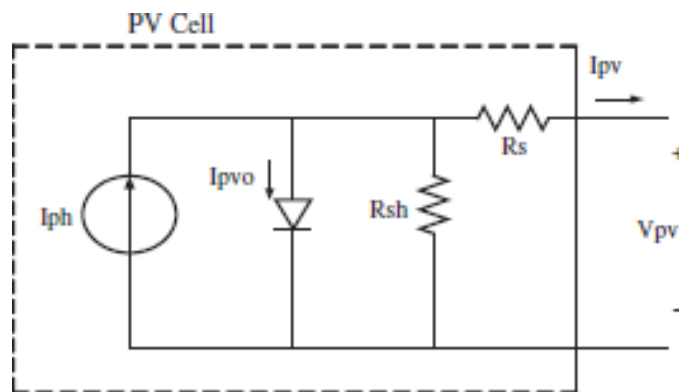Fig. 2. Cp _ k characteristics of the WECS at different pitch angles.

Fig.3. Equivalent circuit of PV cell.

Maximize the ratio of photocurrent to reverse saturation current while minimising series resistance Rs and maximum shunt resistance Rsh within the PV cell to maximise the fill factor. As a result, we can assume that series resistance Rs is close to zero and shunt resistance Rsh is close to infinite, and Eq. (4) can be simplified to be rewritten as follows [7]:

$$I_{PV} = I_{ph} - I_{PVO}\left[\exp\left(\frac{q(V_{PV} + I_{PV}R_s)}{nKT}\right) - |1\right]$$

1.2 MPPT Control for PV systems

Due to the high cost of PV cells, MPPT must be used to keep the voltage close to the maximum power point in a changing environment. The proposed PV systems consist of an array of 4 3 and 4 6 panels, a dc/dc converter, a dc/ac inverter, and a control algorithm, which is typically performed by a microcontroller to continuously track the maximum power. MPPT is also used to ensure that the required load receives a constant voltage [10].

1.3 Perturbation and Observation (P&O) method

The P&O method [2] is the most widely used method in this field. It seeks the maximum power point by periodically increasing or decreasing the voltage of the PV cell, as previously mentioned. In this paper, a variable step method for finding the maximum power point is proposed, in which the step lengths are adjusted based on the distances to the maximum power point (MPP). The step length of duty ratio D, which is actually the slope of each operating point under very short sampling time, is defined as the ratio of variation of power (P) to voltage (V). The control block of the P&O method is shown in Fig. 4.

1.3.1 General Regression Neural Network (GRNN)

a. Generalized regression

Specht proposed the GRNN as a feed-forward neural network training algorithm alternative to the well-known back-error propagation training algorithm. This neural network, like other probabilistic neural networks, requires a small fraction of the training samples required by a back propagation neural network [11, 12]. For a back propagation neural network, the data available from operating system measurements is rarely enough. Because of its ability to converge to the underlying function of the data with only a few training samples, the use of a probabilistic neural network is particularly advantageous. The additional knowledge required to achieve a satisfying fit is minimal, and it can be accomplished without the user's input.
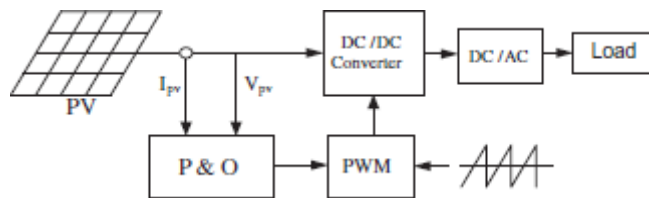

Fig. 4. Block diagram of P&O Method

The normal distribution is the probability density function used in GRNN. The mean of a normal distribution is used for each training sample, Xj.

$$Y(X) = \frac{\sum_{i=1}^{n} Y_i \exp\left[-\frac{D_i^2}{2\sigma^2}\right]}{\sum_{i=1}^{n} \exp\left[-\frac{D_i^2}{2\sigma^2}\right]}$$

$$D_i^2 = (X - X_i)^T (X - X_i)$$

The distance Dj between the training sample and the prediction point is used to determine how well each training sample can represent the prediction X position. exp D2j =2r2 becomes large when the distance Dj between the training sample and the point of prediction is small. When Dj = 0, exp D2j =2r2 becomes one, and this training sample best represents the evaluation point. The separation between all of the other training samples is greater. As the distance Dj grows larger, the term exp D2j =2r2 shrinks, and the contribution of the other training samples to the prediction shrinks as well.

For the jth training sample, the term Yj exp D2j =2r2 is the largest and has a significant impact on the prediction. A search is conducted on the standard deviation, also known as the smoothness parameter r in [11]. For a larger smoothness parameter, a wider range of X is possible for the possible representation of the evaluation point by the training sample. The representation is limited to a narrow range of X, respectively, for a small value of the smoothness parameter.

1.4 Architecture

The controller uses a four-layer GRNN with a boost converter, as shown in Fig. 5, to generate the control law VMPPT, as well as x11 14 VPV, x12 14 IPV, and x13 14 Temperature. The PWM module is used to control the duty cycle of the switch by generating PWM pulses. The general structure of the GRNN is depicted in Fig. 6.

In each GRNN pattern neuron, the calculations are exp D2j =2r2, the normal distribution centred at each training sample. The signals from the pattern neuron I that enter the Denominator neuron are weighted according to the values of the training samples Yi. The signals entering the Numerator neuron have a single weight. Every point predicted by GRNN is influenced by each sample from the training data.

The input vector will be channeled into the GRNN by the input layer, and the distance to the recorded patterns will be calculated in each of the pattern nodes by the pattern layer. The summing operation for the upper and lower parts of (9 is performed by the summation layer, and the final network output is obtained by the output layer, which performs the normalisation function [13,14]. To the output layer, the two summation units Denominator and Numerator, which are given by:
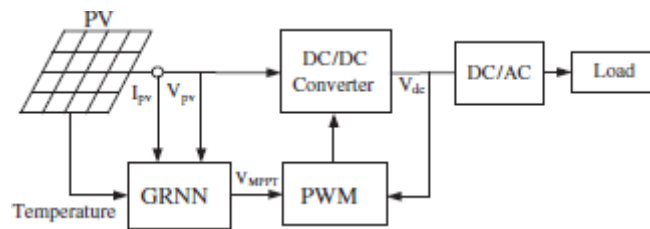

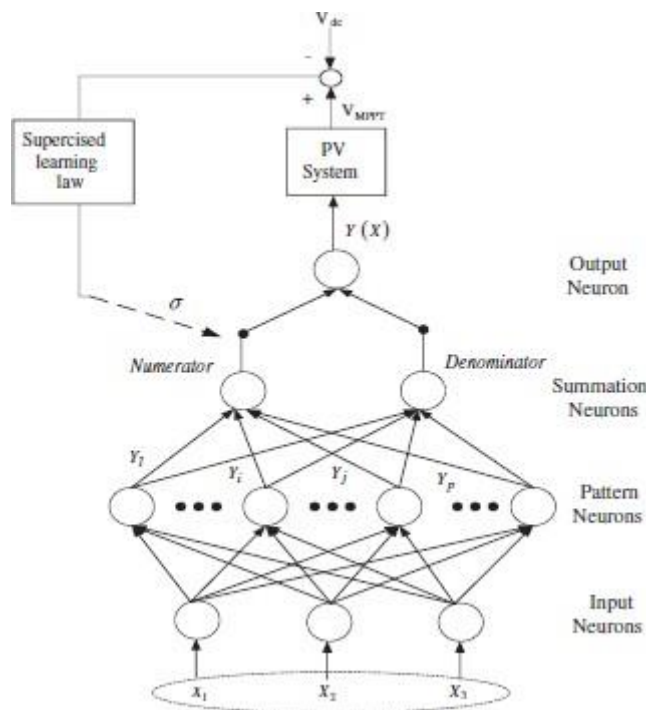*Fig.5. Block diagram of Intelligent MPPT Method.*

Fig. 6. Structure of the four-layer GRNN.

$$\text{Denominator} = \sum_{i=1}^{n} Y_i \exp\left[-\frac{D_i^2}{2\sigma^2}\right], k = 1, 2$$

$$\text{Numerator} = \sum_{i=1}^{n} \exp\left[-\frac{D_i^2}{2\sigma^2}\right]$$

2.   MPPT CONTROL FOR WIND ENERGY SYSTEMS

The proposed pitch angle control system using PI and RBFNSM is explained in this section, and the wind power generation system studied in this paper is shown in Fig.7.

2.1 RBFNSM controller design

Assume the switching function is an RBFN input, the sliding mode controller is the neural network's output, and the RBFNSM control can be built using self-learning [15– 17]. Figure 8 depicts the structure of the RBFNSM controller. The sliding surface is defined as: st 14 cet _et 10 where Pout and Pref represent the generator's actual output power and reference output power, respectively. The tracking error is denoted by the letter e. The iterative algorithm of output weight, central vector of mode, and base width constant can be expressed as follows using the gradient descent algorithm:

$$w_j(t) = w_j(t-1) + \eta[y(t) - y_m(t)]h_j + \alpha[w_j(t-1) - w_j(t-2)]$$

$$\Delta b_j = [y(t) - y_m(t)]w_j h_j \frac{\|X - c_j\|^2}{b_j^3}$$

$$b_j(t) = b_j(t-1) + \eta \Delta b_j + \alpha[b_j(t-1) - b_j(t-2)]$$

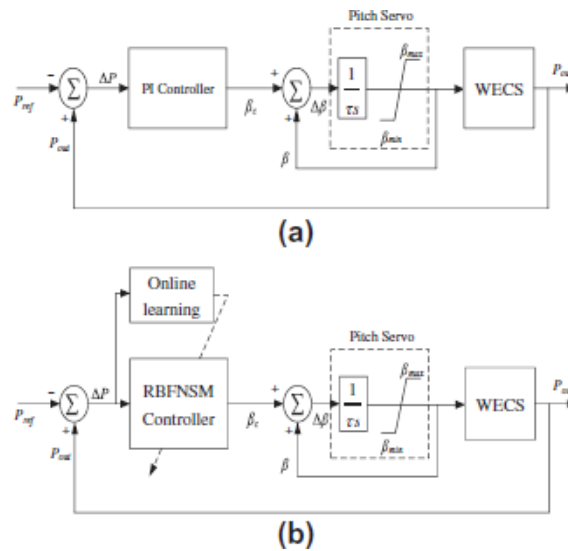**(a)**

(b)

Fig. 7. Pitch control for WECS (a) PI controller and (b) RBFNSM controller
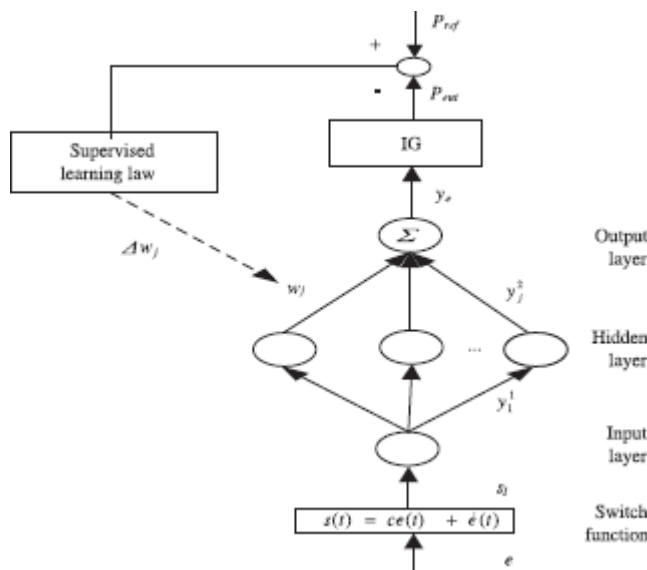
Fig. 8. Architecture of the RBFNSM.

$$\Delta b_{ij} = [y(t) - y_m(t)] w_j \frac{x_j - c_{ij}}{b_j^2}$$

$$c_{ij}(t) = c_{ij}(t-1) + \eta \Delta c_{ij} + \alpha [c_{ij}(t-1) - c_{ij}(t-2)]$$

where an is the momentum factor and g is the adaptive rate. The RBFN's output is the sliding mode controller, and the signal propagation and basic functions in each layer are described in the following sections.

Layer 1: Input layer

The node is defined in the input layer by

$$net_1^1 = s_1^1(k)$$
$$y_1^1(k) = f_1^1(net_1^1(k)) = \left| net_1^1(k) \right|$$

where k denotes the kth iteration and s11 k denotes the switching surface.

Layer 2: Hidden layer

The node is defined in the hidden layer by

$$net_j^2(k) = -\frac{\|s_1^2 - c_j\|^2}{b_j^2}$$
$$y_j^2 = f_j^2\left(net_j^2(k)\right) = \exp\left(net_j^2(k)\right), \quad j = 1, 2, \ldots, m$$

where cj is the jth mode's central vector. bj is the jth mode's base width constant, and bj > 0.

Layer 3: Output layer

The node input and output are represented as in the output layer.

$$net_o^3 = \sum_j w_j y_j^2(k)$$
$$y_o^3(k) = f_o^3\left(net_o^3(k)\right) = net_o^3(k) = \beta_c$$

where y3 o k is the RBFNSM output as well as the proposed controller's pitch angle command. After the RBFNSM has been initialised, the system is trained using supervised learning and gradient descent. The back-propagation algorithm's derivation is the same as this one [18,19]. Using the training patterns, it is used to adjust the RBFNSM's parameters wj, c1j, and b1j. The error term for each layer is calculated and updated using a recursive application of the chain rule. The control objective is set to st st! 0, and the RBFN weight adjustment goal is set to

$$E = s(t)\dot{s}(t)$$

Below is a description of the learning algorithm.

Layer 4: Update weight wj

$$\delta_o = -\frac{\partial E}{\partial net_o^3} = \left[\frac{\partial E}{\partial y_o^3} \frac{\partial y_o^3}{\partial net_o^3}\right]$$

Furthermore, the weight is updated by

$$w_j(t+1) = w_j(t) + \eta_w \Delta w_j$$

where gw denotes the rate of learning.

Layer 5: Update central vector c1j

The update law of c1j is updated using the chain rule. The propagated error term is given by

$$\Delta c_{1j} = -\frac{\partial E}{\partial c_{1j}} = \left[-\frac{\partial E}{\partial net_o^3} \right] \left(\frac{\partial net_o^3}{\partial y_j^2} \right) \left\{ \frac{\partial y_j^2}{\partial c_{1j}} \right\}$$

$$= \delta_o w_j y_j^2 \frac{2(s_1^1 - c_{1j})}{(b_{1j})^2}$$

According to the equation, the central vector c1j is updated.

$$c_{1j}(t+1) = c_{1j}(t) + \eta_c \Delta c_{1j}$$

The learning rate is denoted by gc.

Layer 6: Update base width b1j

Wij's update legislation is updated utilising the chain rule.

$$\Delta b_{1j} = -\frac{\partial E}{\partial b_{1j}} = \left[-\frac{\partial E}{\partial net_0^3} \right] \left(\frac{\partial net_0^3}{\partial y_j^2} \right) \left\{ \frac{\partial y_j^2}{\partial b_{1j}} \right\}$$

$$= \delta_o w_j y_j^2 \frac{2(s_1^1 - c_{1j})^2}{(b_{1j})^3}$$

According to the following equation, the base width b1j is updated.

$$b_{1j}(t+1) = b_{1j} + \eta_b \Delta b_{1j}$$

where gb denotes the rate of learning.

3.   RESULTS OF SIMULATION

In the Matlab/ Simpower environment, the hybrid system described in Fig. 1 is implemented. Table 1 shows the WECS parameters as well as the PV array used in the simulation. Many tests were carried out to demonstrate the model's performance under various settings, including a comparison of various MPPT schemes [20–24], including the standard PI and P&O methods.

3.1 Performance of the MPPT system

3.1.1 Wind power MPPT

For the hybrid power system with constant load and sufficient wind and irradiation, a time domain simulation was done. Figure 9 depicts the output power of WECS. Figure 9 shows that the RBFNSM controller has greater control performance than the PI controller, with less transient and smaller vibrations. The transient response at the starting point clearly shows that PI oscillates more than RBFNSM, which oscillates relatively minimally. 1.86 kW is the average power. It increases by 5.7 percent as compared to the PI control.

3.1.2 PV power MPPT

Figure shows the PV output power. As shown in Fig., the GRNN controller outperforms the P&O controller in terms of both transient and stability. 2.3 kW is the average power. It rises by 15% as compared to P&O's. The GRNN approach can track the maximum power output of a PV array rapidly and accurately.

3.2 MPPT with load change

The RBFNSM and PI pitch controllers are used for comparison, they can quickly and accurately track the maximum power output as shown in Table.

| Wind induction generator	
Rated power (kW)	2 and 4
Voltage (V)	220
Frequency (Hz)	60
Inertia	0.7065
No of pole pairs	2
Wind speed (m/s)	8−12
PV array	
Maximum power of module unit (W)	200.143, 25 °C, 1000 W/m^2
Module number	12 and 24
Total power rating (kW)	2.4 and 4.8
Unit rated voltage (V)	26.3
Unit rated current (A)	7.61
Irradiance level (W/m^2)	600−1000
Load	
Capacity (kW)	8−25
Grid	
Voltage (V)	220
Frequency (Hz)	60
Phase	3

Table no. 1. Simulation Parameters.
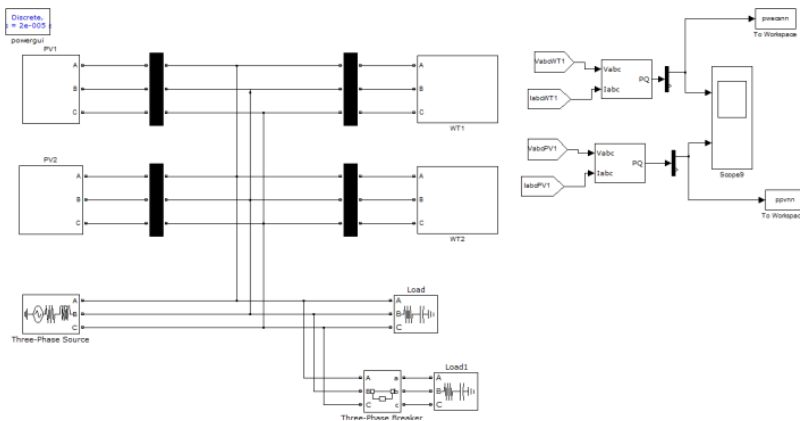
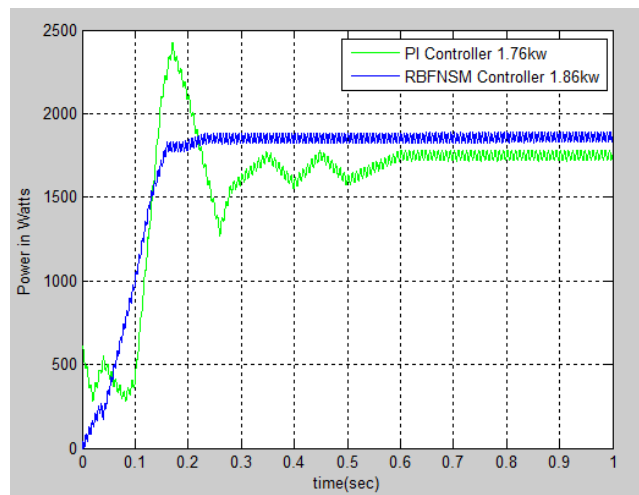**Fig 9 Matlab Simulink model of the proposed system**

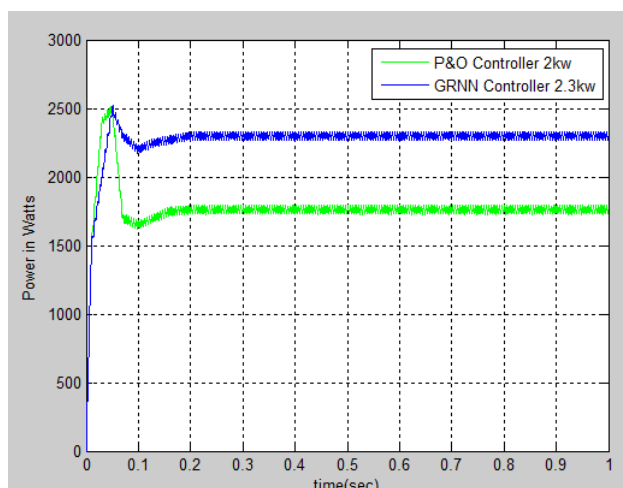*Fig. 10 MPPT tracking response of the WECS.*

Fig. 11 MPPT tracking response of the PV system

Figure 9. Figure 10 displays a comparison of GRNN and P&O methods used in PV power system MPPT. Both can quickly obtain steady power production, but GRNN outperforms P&O. Under load disturbances, the proposed approach may track faster with a more consistent output power.

3.3 under fluctuating load, power management

At 2.5 seconds, the inductive load shifted from 8 kW to 16 kW. When the PV and wind turbine active output power is insufficient, active power is delivered from the grid. Figure 5 depicts the active power output from a grid-connected hybrid generation system. The hybrid power system soon settles into a steady state of operation. As seen in Fig. 5, the system bus voltage has reduced to roughly 0.97 Pu. Under variable load conditions, the proposed approach can track with a more stable output power.

3.4 MPPT in a variety of situations

The WT1 and WT2 wind speeds have been altered from 12 to 8 m/s, the PV1 and PV2 irradiance levels have been modified from 1000 to 600 W/m2, and the total load is 8 kW in this scenario. At 0.5 s, a time domain simulation of the hybrid power system with constant load was done under various wind and irradiance conditions.

CONCLUSION

Natural processes continuously replenish renewable energy sources, often known as non- conventional energy. Hybrid systems are the best option for producing renewable energy. A new wind-PV hybrid generation system has been designed and implemented in this paper. Four case studies illustrate that voltage and power in a hybrid system can be well regulated in a changing environment. MATLAB/Simulink was used to create the simulation model for the hybrid generation system.

To extract the greatest power from the wind and solar energy sources, this grid-connected hybrid generation system can fully exploit the characteristics of the proposed wind generator and PV panels. The GRNN and RBFNSM algorithms can track the maximum power output of a hybrid power system rapidly and accurately. Furthermore, efficient power sharing among energy sources has been successfully proven with increased efficiency, improved transient, and increased stability, even under varying load situations and disturbances.

REFERENCES

[1]   Cheng YM, Liu YC, Hung SC, Cheng CS. Multi-input inverter for grid-connected hybrid PV/wind power system. IEEE Trans Power Electron 2007; 22(3):1070–6.

[2]   Femia N, Petrone G, Spagnuolo G, Vitelli M. Optimization of perturb and observe maximum power point tracking method. IEEE Trans Power Electron 2005; 20(4):963–73.

[3]   Morimoto S, Nakamura T, Sanada M, Takeda Y. Sensorless output maximization control for variable-speed wind generation system using IPMSG. IEEE Trans Ind Appl 2005;41(1):60–7.

[4]   Bakic V, Pezo M, Stevanovic Z, Zivkovic M, Grubor B. Dynamical simulation of PV/Wind hybrid energy conversion system. Energy 2012;45(1):324–8.

[5]   Dursun E, Kilic O. Comparative evaluation of different power management strategies of a stand-alone PV/Wind/PEMFC hybrid power system. Int J Elect Power Energy Syst 2012;34(1):81–9.

[6]   Giraud F, Salameh ZM. Steady-state performance of a grid connected rooftop hybrid wind–photovoltaic power system with battery storage. IEEE Trans Energy Convers 2001;16(1):1–7.

[7] Kwon JM, Kwon BH, Nam KH. Three-phase photovoltaic system with three level boosting MPPT control. IEEE Trans Power Electron 2008;23(5):2319–27.

[8] Chen CH, Hong CM, Cheng FS. Intelligent speed sensor less maximum power point tracking control for wind generation system. Int J Elect Power Energy Syst 2012;4234(1):399–407.

[9] Kellogg WD, Nehrir MH, Venkataramanan G, Greez V. Generation unit sizing and cost analysis for stand-alone wind, photovoltaic, and hybrid wind/PV systems. IEEE Trans Energy Convers 1998;13(1):70–5.

[10] Ghassami AA, Sadeghzadeh SM, Soleimani A. A high performance maximumpower point tracker for PV systems. Int J Elect Power Energy Syst 2013;53:237–43.

[11] Specht DF. Probabilistic neural network for classification, mapping, or associative memory. Proc IEEE Int Conf Neural Network 1988;1:525–32.

[12] Specht DF. Generation of polynomial discriminant functions for pattern recognition. IEEE Trans Electron Comput 1967;EC-16:308–19.

[13] Parzen E. On estimation of a probability density function and mode. Ann Math Statistics 1962;33:1065–76.

[14] Kenji NF, Anna DPL, Carlos RM. Short-term multinodal load forecasting using a modified general regression neural network. IEEE Trans Power Delivery

[15] 2011;26(4):2862–9.

[16] Lin WM, Hong CM. A new Elman neural network-based control algorithm for adjustable-pitch variable speed wind energy conversion systems. IEEE Trans Power Electron 2011;26(2):473–81.

[17] Caoullos T. Estimation of a multivariate density. Ann Inst Statistics Math 1966;18(2):179–89.

[18] Lin SC, Park JK. RBF network based sliding mode control. In: IEEE international conference on systems, man, and, cybernetics; 1998. p. 1957–61.

[19] Munoz D, Sbarbaro D. An adaptive sliding-mode controller for discrete nonlinear systems. IEEE Trans Indust Electron 2000:574–81.

[20] Seshagiri S, Khail HK. Output feedback control of nonlinear systems using RBF neural networks. IEEE Trans Neural Network 2000;11:69–79.

[21] Mohammadi M, Nafar M. Fuzzy sliding-mode based control (FSMC) approach of hybrid micro-grid in power distribution systems. Int J Elect Power Energy Syst 2013;51:232–42.

[22] Wang Q, Chang L. An intelligent maximum power extraction algorithm for inverter- based variable speed wind turbine systems. IEEE Trans Energy Convers 2004;19(5):242– 1249.

[23] Payman A, Pierfederici S, Meibody-Tabar F. Energy management in a fuel cell/supercapacitor multisource/multiload electrical hybrid system. IEEE TransmPower Electron 2009;24(12):2681–91.

[24] Wang C, Nehrir MH. Power management of a stand-alone wind/photovoltaic/ fuel cell energy system. IEEE Trans Energy Convers 2008;23:957–67.

[25] Liu S, Dougal RA. Dynamic multiphysics model for solar array. IEEE Trans Power Electron 2002;17(2):285–94.